Available online at www.sciencedirect.com
ScienceDirect
Tetrahedron 62 (2006) 9156–9165
Tetrahedron

Synthesis, crystal structures and the preliminary evaluation of the new dibenzotetraaza[14]annulene-based DNA/RNA binding agents

Dariusz Pawlica,[a] Marijana Radić Stojković,[b] Lesław Sieroń,[c] Ivo Piantanida[b] and Julita Eilmes[a,*]

[a]*Department of Chemistry, Jagiellonian University, Ingardena 3, 30-060 Kraków, Poland*
[b]*Laboratory for Supramolecular and Nucleoside Chemistry Ruđer Bošković Institute, PO Box 180, HR-10002 Zagreb, Croatia*
[c]*Institute of General and Ecological Chemistry, Technical University of Łódź, Żeromskiego 116, 90-924 Łódź, Poland*

Received 6 April 2006; revised 23 June 2006; accepted 13 July 2006
Available online 7 August 2006

Abstract—A series of water-soluble dicationic dibenzotetraaza[14]annulenes have been prepared in order to examine their interactions with nucleic acids. Pendant water-solubilizing *N*-pyridinium, 4,4′-bipyridinium and *N*-methyl pyridinium moieties have been attached to the central core via linkers generated by direct N-alkylations and ester creating couplings, respectively. The crystal structures of derivatives equipped with 3-(*N*-pyridinium-1-yl)propyl and 3-(4,4′-bipyridinium-1-yl)propyl substituents have been determined. Interactions with *ct*-DNA have been studied and evidenced by means of spectrophotometric titrations with Scatchard analysis and thermal denaturation experiments.

1. Introduction

Dibenzotetraaza[14]annulenes (Fig. 1) are among the most extensively studied synthetic macrocycles.[1] The attention which has been focused on these macrocyclic compounds arose mainly from their resemblance to porphyrins, and consequently, from their relevance in bioinorganic chemistry[2] and materials science.[3] Similarly to porphyrins, they have four coplanar nitrogen donor atoms and a number of double bonds with substantial π delocalization (benzenoid rings and 1,3-diiminato fragments). Unlike porphyrins, dibenzotetraaza[14]annulenes are Hückel anti-aromatic (4*n*) and have a 14-membered inner ring as compared to the larger 16-atom inner porphyrin ring.[4] It is of importance for the potential applications of dibenzotetraaza[14]annulenes that they are relatively easy to synthesize,[5] highly reactive at the *meso* positions[6] and capable of accommodating various substituents on the phenylene rings and diimine carbons. In addition, crystallography reveals that they adopt various conformations ranging from planar to saddle shaped, depending on the ring substitution.[7] Accordingly, as ligands for transition metals and main group elements, they offer a wide variety of coordination modes and geometries.[7] Thus it appears that the structure and properties of dibenzotetraaza[14]annulenes can easily be tuned through the careful choice of peripheral substituents and inserted metal ions. They therefore seem to be very attractive for the design and synthetic elaboration of tailor-made drugs for biomedical applications.

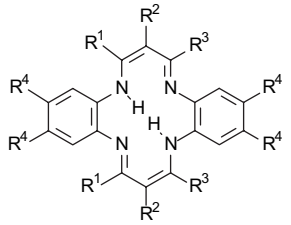

Figure 1.

In this paper we report on the preparation, structure and preliminary evaluation of novel dibenzotetraaza[14]annulene-based DNA/RNA binders. There is no data, as of yet, in the literature on the similar applications of dibenzotetraaza[14]annulenes. In contrast, porphyrins, to which they are often compared, belong to the most often and successfully explored systems in this area, capable of interacting with DNA via intercalation, minor/major groove binding[8] as well as in some cases through outside binding of self-stacked helically organized porphyrin oligomers.[9] Also other macrocycles and their metal complexes have been widely employed in studies focused on similar biomedical applications.[10]

Keywords: Dibenzotetraaza[14]annulenes; Water-solubilizing groups; Synthesis; Crystal structure; DNA binding; UV–vis titration; DNA thermal denaturation.
* Corresponding author. Tel.: +48 12 6632294; fax: +48 12 6340515; e-mail: jeilmes@chemia.uj.edu.pl

0040–4020/$ - see front matter © 2006 Elsevier Ltd. All rights reserved.
doi:10.1016/j.tet.2006.07.045

We have chosen the β-unsubstituted macrocycles, known for their planar conformation,[11] as the central core of potential DNA intercalators/binding agents. Water-solubilizing cationic groups based on pyridinium and bipyridinium moieties have been linked to the main framework through spacers of variable lengths, flexibility and chemical characteristics. The molecules thus designed possess appropriate molecular sizes, planar chromophores and positively charged centres at the ends of the side chains linked to the *meso* positions. They are therefore expected to offer diverse modes of supramolecular interactions with nucleic acids. First of all, the central flat part of these molecules can insert and stack between base pairs of double helical DNA, in this function they can resemble porphyrin-based DNA binders. Pendant cationic residues that are important for generating water solubility provide centres of electrostatic and cation to π supramolecular interactions. They are independent, in fact, from the central planar core since the linkers are mainly aliphatic, relatively long and flexible. External electrostatic interactions between cationic moieties and anionic phosphate backbone can also be expected, as well as additional noncovalent forces generated by ester-function-containing linkers. A question arises also as to whether dibenzotetraaza[14]annulene derivatives will exhibit a tendency of self-aggregation on the nucleic acids backbone, similarly to their porphyrin analogs.[9] It seems reasonable to expect that features that make dibenzotetraaza[14]annulenes different from porphyrins (i.e., smaller coordination cavity size, anti-aromaticity and flexibility of the ring) will be of significance in modifying their interactions with nucleic acids, as compared to their porphyrin-based analogues.

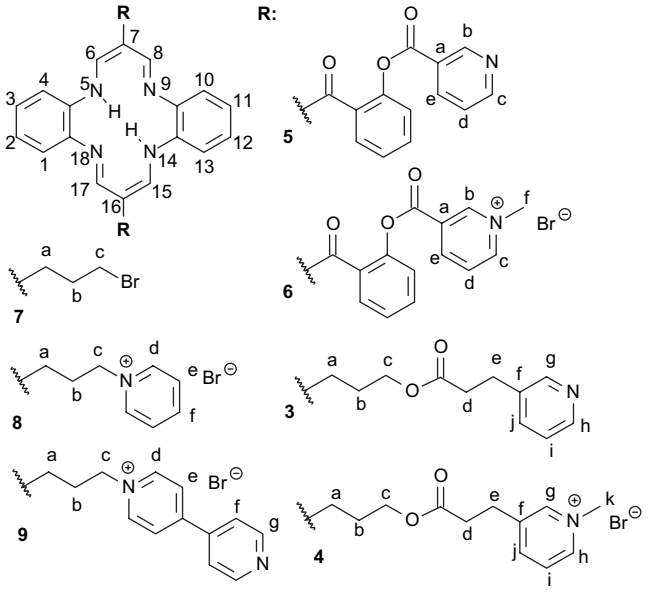

Figure 2. Potential DNA/RNA binding agents **4**, **6**, **8** and **9**, and other new derivatives of dibenzotetraaza[14]annulene.

Finally, it is relevant to note that the possible metallation of these new macrocyclic ligands with various metal ions can give rise to complexes with new metal-centre-dependent properties, such as specificity in targeting DNA sites. Appropriately chosen central metal ions may allow the preparation of complexes able to selectively break DNA strands.[12]

Potential DNA/RNA binding agents **4**, **6**, **8**, **9** and other new derivatives of dibenzotetraaza[14]annulene synthesized in this work are shown in Figure 2. Scheme 1 outlines the reactions performed.

2. Results and discussion

2.1. Synthesis

To synthesize water-soluble dicationic products **4**, **6**, **8** and **9** we have used dibenzotetraaza[14]annulenes **1**[13] and **2**[14] as substrates and employed the reactivities of OH groups at their *meso* substituents. Thus, ester-linkages-creating couplings between the OH groups of **1** and COOH group of 3-pyridinepropionic acid allowed 3-hydroxypropyl of **1** to be transformed into 3-(3-pyridyl)propionyloxypropyl. Similarly, the phenolic OH groups of the substrate **2** have been esterified by means of nicotinic acid to give corresponding

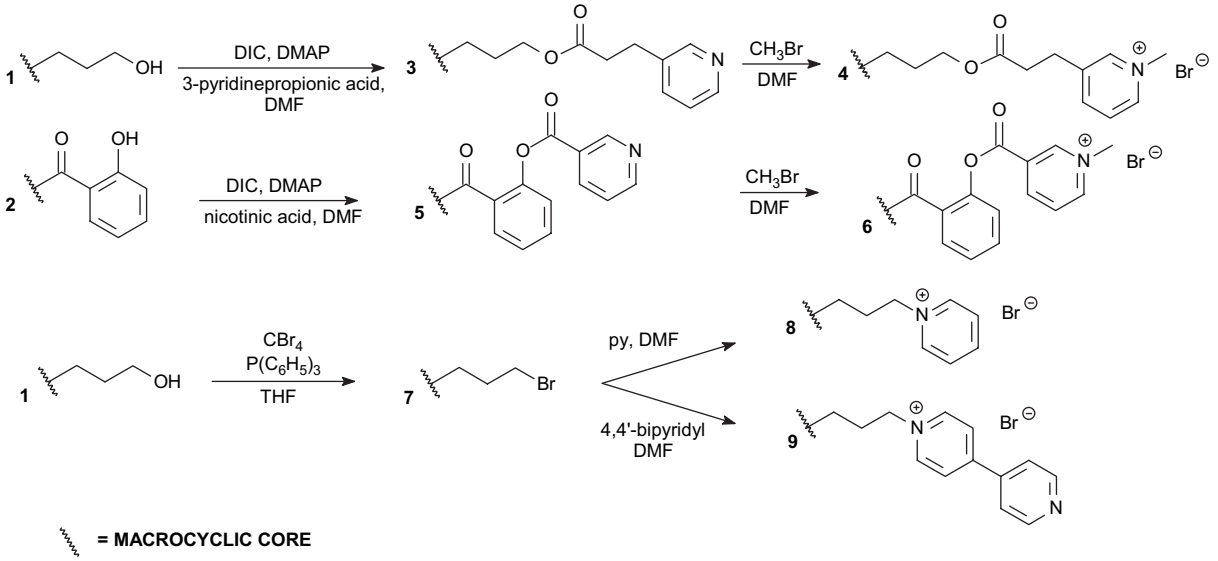

Scheme 1.

(3-pyridyl)carbonyloxybenzoyl derivatives. Coupling procedures using diisopropylcarbodiimide (DIC) as a dehydrating agent[15] and dimethylaminopyridine (DMAP) as an acylation catalyst[16] were successfully employed in both cases affording products **3** and **5** in fair yields of 72% and 87%, respectively. In the next steps, **3** and **5** have been methylated by means of bromomethane giving **4** and **6** in yields of 75% and 81%, respectively.

To synthesize dicationic products **8** and **9**, substrate **1** has been transformed to **7** with the use of a PPh_3–CBr_4 mixture.[17] Bis(bromopropyl)dibenzotetraaza[14]annulene **7** was then reacted with pyridine and 4,4′-bipyridine to give **8** and **9** in reasonable yields of 63% and 71%, respectively.

All new products have been characterized by elemental analysis, ^{1}H and ^{13}C NMR, ESI-MS and IR data. ^{1}H and ^{13}C NMR signals with their assignments and other spectroscopic and analytical data are collected in Section 4.

2.2. Crystallography

The structures of compounds **8** and **9** with the atomic numbering scheme are shown in Figures 3 and 4. Crystal data and structural refinement details are given in Table 1.

Both compounds crystallize in the $P2_1/c$ space group with two molecules per unit cell. The central 14-membered ring of the macrocyclic cation of each compound has a planar conformation and lies across a centre of inversion. The macrocyclic rings are not ideally planar. The distortion from planarity is up to 0.45(2) Å for N1 atom of **8**, and 0.044(2) Å for C7 atom of **9**.

The difference in the Fourier map analysis of **8** exhibited two peaks located in the expected positions of H amine atoms that refer to the separation between the two half-proton positions and indicate the presence of two tautomeric states of a tetraaza[14]annulene ring.[11c] In the structure of **9** at 90 K, only one peak corresponding to the H amine atom was found. The aliphatic chains in both compounds adopt nearly planar extended conformations with torsion angles: C9–C10–C11–C12 of 178.0(2)° and 174.8(3)°, and C10–C11–C12–N3 of −169.7(2)° and 167.4(2)° for **8** and **9**, respectively. In the crystal structure of **9**, the bipyridinium moiety is slightly twisted, with an interplanar angle of 9.9(1)° between the two pyridine rings.

The supramolecular structure of compound **8** is defined by C–H···Br, C–H···π and π···π stacking interactions between the ions, as shown in Figure 5. The two π···π-bonded

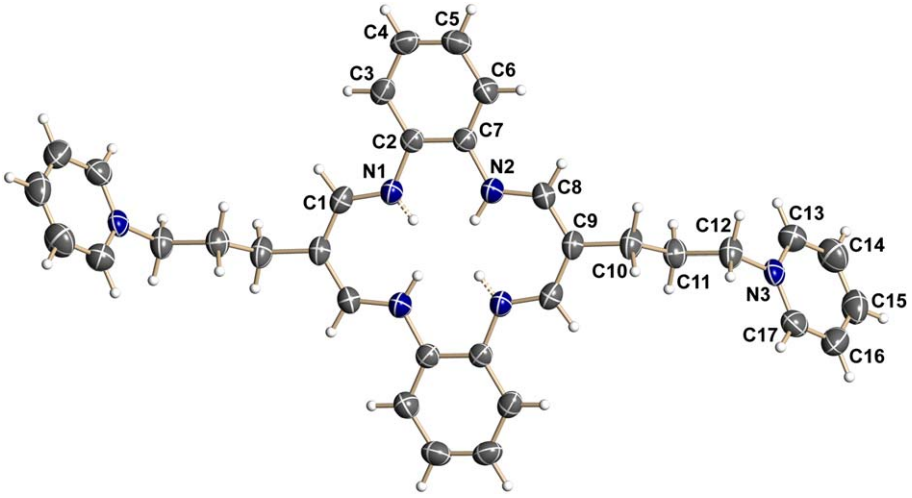

Figure 3. The structure of macrocyclic cation of **8** at 290 K, showing 50% probability displacement ellipsoids with the atom numbering scheme.

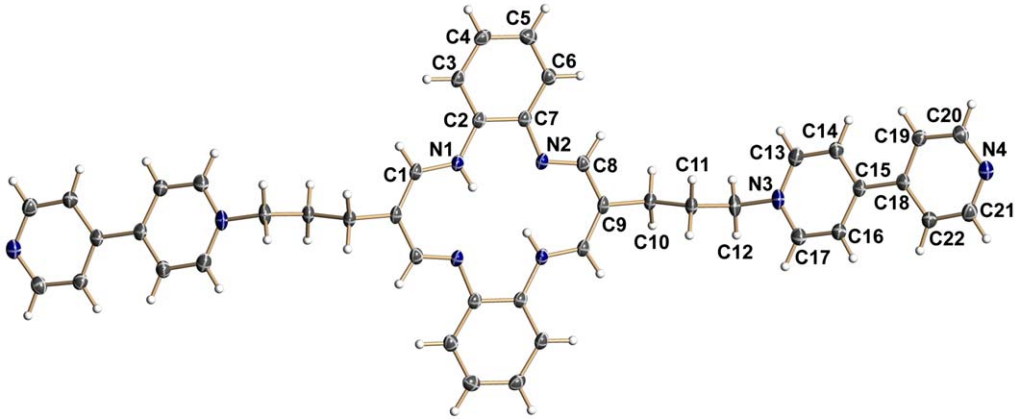

Figure 4. The structure of macrocyclic cation of **9** at 90 K, showing 50% probability displacement ellipsoids with the atom numbering scheme.

Table 1. Crystal data and structural refinement details for **8** and **9**

	8	**9**
Empirical formula	$C_{34}H_{36}N_6^{2+}\cdot 2Br^-$	$C_{44}H_{42}N_8^{2+}\cdot 4H_2O\cdot 2Br^-$
Formula weight	688.49	914.74
Crystal system	Monoclinic	Monoclinic
Space group	$P2_1/c$	$P2_1/c$
a (Å)	14.0767(14)	7.6302(2)
b (Å)	8.3116(9)	18.7942(4)
c (Å)	15.4211(17)	14.8324(3)
β (°)	122.314(11)	101.1100(10)
V (Å^3), Z	524.8(3), 2	2087.16(8), 2
d_{calc} (g/cm^3)	1.500	1.456
F(000)	704	944
Temperature (K)	290	90
Radiation type, wavelength (Å)	Mo Kα, 0.71073	Cu Kα, 1.54178
Absorption coefficient (mm^{-1})	2.693	2.893
Theta range (°)	2.64–25.00	3.84–69.98
Limiting indices, h, k, l	$-16\rightarrow13$, $-9\rightarrow9$, $-16\rightarrow16$	$-8\rightarrow9$, $-22\rightarrow22$, $-17\rightarrow18$
Reflections collected	6887	22623
Independent reflections	2514	3935
Data/restraints/parameters	2514/190/0	3935/282/5
Goodness-of-fit on F^2	1.000	1.093
Final R indices [$I>2\sigma(I)$]	R=0.0315, wR^2=0.0901	R=0.0474, wR^2=0.1363
Final R indices [all data]	R=0.0402, wR^2=0.0925	R=0.0475, wR^2=0.1364
Largest diff. peak and hole ($e\cdot$Å^{-3})	0.39, −0.49	1.36, −1.20

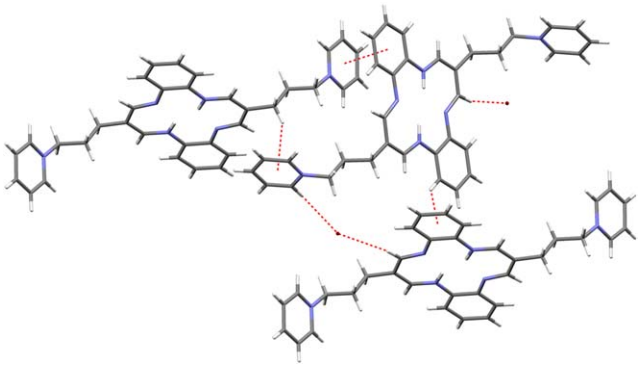

Figure 5. The intermolecular C–H···Br, C–H···π and π···π stacking interactions in **9**, shown as dashed lines.

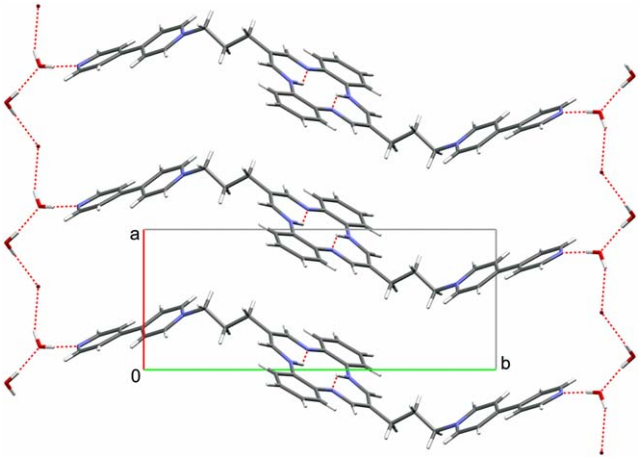

Figure 6. The one-dimensional hydrogen-bonded ladder motif in **9**, running along the *a*-axis.

benzene rings N3/C(13–17) and C(2–7) are almost fully eclipsed with a centroid–centroid distance of 3.446(2) Å. The results agree well with the recent reports showing that in the absence of strong hydrogen-bond donors, C–H···π and π···π interactions often play an important role in the supramolecular assembly of aromatic compounds.[18]

In contrast, structure **9** is stabilized mainly by a network of O–H···N, O–H···O and O–H···Br hydrogen bonds. Hydrogen bonds involving water molecules and bromide anions lead to the formation of infinite one-dimensional chains. The cation moieties link these chains via O–H···N hydrogen bonds in a supramolecular ladder motif, running along the *a*-axis, as represented in Figure 6.

The hydrogen-bond interactions observed in the structures are summarized in Table 2.

2.3. UV–vis spectroscopy, binding to *ct*-DNA

Compounds **4**, **6**, **8** and **9** are moderately soluble in pure water and somewhat less in an aqueous buffered system (in the range of $c=1\times10^{-3}$ mol dm^{-3}), probably due to the higher ionic strength. The UV–vis tests showed compounds **4**, **8** and **9** to be stable in an aqueous solution within the temperature range of 25–90 °C for at least one week, whereas the spectrum of the freshly prepared aqueous solution **6** substantially changed over the time, even in deoxygenated conditions. Since no precipitation was observed, and solution **6** was stable in the dark, the chemical decomposition of **6** was most likely taking place under UV–vis irradiation. A structure comparison of unstable **6** and stable **4**, **8** and **9** suggested that the aromatic ester bonds of **6** were decomposing. The product **6** was therefore not used in further studies. The UV–vis absorbance of buffered aqueous solutions of **4**, **8** and **9** was proportional to their concentration up to 5×10^{-5} mol dm^{-3}, indicating no significant intermolecular stacking. Absorption maxima of **4**, **8** and **9** and the corresponding molar extinction coefficients are given in Table 3.

The interactions of **4**, **8** and **9** with *ct*-DNA were examined by spectrophotometric titrations and thermal denaturation experiments, exemplified by Figures 7 and 8, respectively.

Table 2. The hydrogen-bond interactions (Å, °)

D–H···A	H···A	D···A	∠ D-H···A	Symmetry code (#)
8				
N1–H2′···N2$^{\#}$	2.12	2.758(3)	131	$-x$, $-y+1$, $-z+1$
N2–H2···N1$^{\#}$	2.11	2.758(3)	132	$-x$, $-y+1$, $-z+1$
C1–H1···Br1$^{\#}$	2.87	3.713(3)	151	$-x$, $-y+1$, $-z+1$
C13–H13···Br1$^{\#}$	2.99	3.890(2)	162	x, $-y+½$, $z-½$
C6–H6···C_g(1)$^{\#}$	3.04	3.817(3)	142	$-x$, $y-½$, $-z+½$
C10–H10B···C_g(1)$^{\#}$	2.89	3.711(3)	143	$-x+1$, $y-½$, $-z+^3/_2$
9				
N1–H1···N(2)$^{\#}$	2.11	2.788(3)	133	$-x$, $-y+1$, $-z$
O1–H01···Br1$^{\#}$	2.54	3.381(2)	177	$-x+1$, $y+½$, $-z+½$
O1–H102···O2$^{\#}$	1.87	2.699(4)	172	$x+1$, y, z
O2–H201···N4$^{\#}$	1.99	2.818(4)	170	x, $-y+½$, $z-½$
O2–H202···Br1$^{\#}$	2.53	3.310(3)	154	$-x+1$, $y+½$, $-z+½$
C10–H10A···C_g(2)$^{\#}$	2.60	3.362(3)	134	$-x+1$, $y+½$, $-z+½$

C_g(1)=N3/C13/C14/C15/C16/C17; C_g(2)=C2/C3/C4/C5/C6/C7.

Table 3. Electronic absorption maxima and corresponding molar extinction coefficients of **4**, **8** and **9**[a]

	λ_{max}/nm	$\varepsilon\times10^3$/dm^3 mol^{-1} cm^{-1}
4	265	28.6
	383	34.6
	443	11.3
	447	11.2
8	263	29.79
	379	34.88
	427	12.29
9	258	49.67
	385	25.53
	431	11.45
	448	11.62

[a] Sodium cacodylate buffer, I=0.05 mol dm^{-3}, pH=7.

Titration data were processed according to Scatchard equation.[19] The results of all experiments are collected in Table 4.

The addition of *calf thymus* (*ct*)-DNA yielded strong bathochromic and hypochromic effects in UV–vis spectra of **4** and **8** (Fig. 7, Table 4) but only very weak changes in the UV–vis spectrum of **9** (Table 4). Binding constants (log K_s) and ratios n (Table 4) calculated by Scatchard equation can be considered only as the cumulative values since deviation from the isosbestic points in UV–vis titrations can be observed (Fig. 7), which implies the co-existence of various types of complexes.

In thermal denaturation experiments, the addition of **4** and **8** stabilized the *ct*-DNA double helix, whereas the addition of **9** again did not show any measurable impact on the *ct*-DNA melting temperature. The stabilizing influence of **8** was found to be higher than that of **4**.

One could expect that, similarly to the porphyrins, dibenzotetraaza[14]annulenes **4**, **8** and **9** would base their interactions with DNA on intercalation and/or minor/major groove binding. As inferred from the experiments depicted above, only **4** and **8** exhibited pronounced interactions with the *ct*-DNA. Strong bathochromic and hypochromic changes in the UV–vis spectra of **4** and **8** pointed towards aromatic

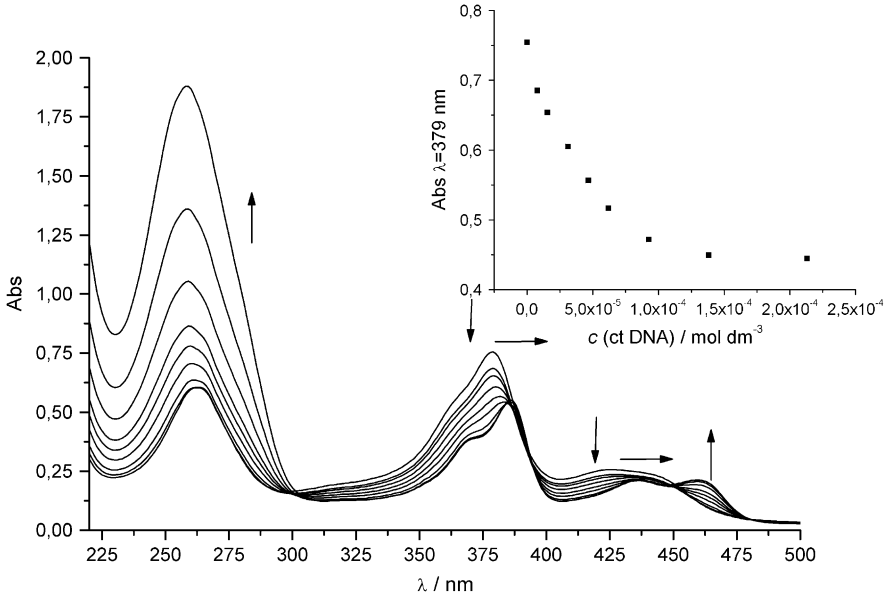

Figure 7. Changes in UV–vis spectrum of **8** (c=2.06×10^{-5} mol dm^{-3}) upon titration with *ct*-DNA and dependence of **8** absorbance at λ_{max}=379 nm on c (*ct*-DNA), at pH=7, sodium cacodylate buffer, I=0.05 mol dm^{-3}.

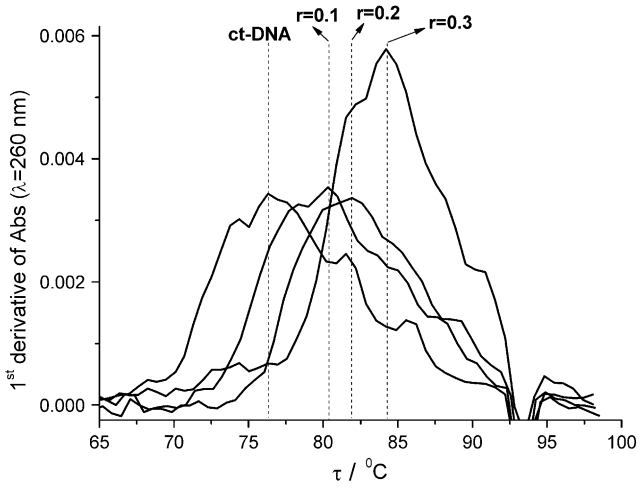

Figure 8. Thermal denaturation experiments of *ct*-DNA and **8** at pH=7.0 (sodium cacodylate, I=0.05 mol dm^{-3}), the ([**8**]/[*ct*-DNA]) ratios (r) are 0.0, 0.1, 0.2 and 0.3. For measuring conditions, see Section 4.

stacking interactions with *ct*-DNA,[20,21] which together with the thermal stabilization of the *ct*-DNA gave evidence of an intercalative mode of binding. However, systematic deviation from the isosbestic points in the UV–vis titrations of **4** and **8** as well as values of ratio n (Table 4) far too high for intercalation, indicate the simultaneous formation of various types of complexes. Therefore the binding of **4** and **8** into one of the DNA grooves and/or on the outer surface of the polynucleotide cannot be neglected.

The question arises, in turn, as to why, unlike **4** and **8**, compound **9** exhibited very weak (if any) interactions with the *ct*-DNA. A comparison of the structures suggests that differences in the binding affinities of **4** and **8**, in relation to those of **9**, depend mainly on the size, rigidity and chemical constitution of their pendant *meso* substituents. Compounds **4**, **8** and **9** have analogous dicationic structures and possess an identical dibenzotetraaza[14]annulene core but the exposure of the positive charges and the bulkiness of their substituents differ significantly. The bipyridinium-containing substituents of **9** are more rigid and bulky than those attached to **4** and **8**. It seems reasonable to suppose that intercalative and groove-binding abilities of **9** have been suppressed due to steric hindrance created by its *meso* substituents.

Table 4. Changes of **4**, **8**, **9** UV–vis spectra upon titration with *ct*-DNA, binding constants ($\log K_s$) and ratios $n_{([\text{bound compound}]/[ct\text{-DNA}])}$ calculated from the UV–vis titrations;[a] and ΔT_m values[f] (°C) of *ct*-DNA upon the addition of **4**, **8** and **9**

	[b]$\Delta\lambda_1$	[b]$\Delta\lambda_2$	[c]H/%	$\log K_s$	[d]n	[f]ΔT_m (°C)
4	+2	+8	−35	5.2	0.69	+2.1
8	+7	+9	−46	4.7	0.84	+7.2
9	0	+2	−8	[e]	[e]	0

Experimental conditions: pH=7.0 (sodium cacodylate buffer, I=0.05 mol dm^{-3}).

[a] Titration data were processed according to Scatchard equation.[19]

[b] Shift of the absorbance maximum; $\Delta\lambda=\lambda$(**4**, **8** and **9**)$-\lambda$(complex); Absorbance maxima λ_1 (**4**: λ=383 nm, **8**: λ=379 nm, **9**: λ=385 nm) λ_2=(**4**: λ=443 nm, **8**: λ=427 nm, **9**: λ=448 nm).

[c] Hypochromic effect; H=[Abs(**4**, **8**, **9**)−Abs(complex)]/Abs(**4**, **8** and **9**)×100; values Abs(complex) were calculated by Scatchard equation[19] for **4** and **8** and the last experimental values were used for the Abs(complex) of **9**.

[d] Accuracy of n±10–30%, consequently $\log K_s$ values vary in the same order of magnitude.

[e] Not possible to calculate by using Scatchard equation due to the small spectroscopic changes.

[f] Error in ΔT_m: ±0.5 °C; $r_{[\text{compound}]/[ct\text{-DNA}]}$=0.3.

It seems noteworthy to mention that the reasoning presented here agrees well with the results reported earlier for closely related analogues of the porphyrin.[21,22] Namely, for less substituted porphyrin (P2 corresponding to **4** and **8**) the increase in ΔT_m reflected the stabilization of the double helix due to the intercalation of the porphyrin moiety,[21,22] while results for more sterically congested analogues (P3 and P4 corresponding to **9**) supported an outside binding mode.[21]

It is difficult at this stage to explain why **8** and **4** differ so much in their stabilizing influence on the *ct*-DNA melting temperatures. Since structures **4** and **8** are quite similar, as well as the observed hypo- and bathochromic effects and obtained log K_s values, one could speculate that the spatial orientation of terminal groups with positive charges could be of decisive importance. A much more detailed study is needed, however, in order to support this assumption.

3. Conclusions

A new class of DNA/RNA binding agents based on the dibenzotetraaza[14]annulene backbone has been synthesized by the chemical transformations within its *meso*-substituted functional groups. The reaction sequence involved esterifications with 3-pyridinepropionic and nicotinic acids, followed by the N-alkylation of the pyridine moieties. Alternatively, the bis(bromopropyl)dibenzotetraaza[14]annulene has been synthesized from a corresponding hydroxypropyl substrate, followed by reactions with pyridine and 4,4′-bipyridine.

X-ray crystallography showed a nearly planar macrocyclic core in **8** and **9** with aliphatic chains adopting extended planar conformations. Terminal groups of the pendant *meso* moieties were found to play a significant role in the supramolecular assembly of **9** arranged in ladder-like motifs.

Spectrophotometric titrations with the use of the Scatchard analysis and the thermal denaturation experiments showed products **4** and **8** to be capable of strong interactions with *ct*-DNA. A mixed mode of binding is proposed involving intercalation and groove binding, both influenced remarkably by the bulkiness and rigidity of the pendant *meso* substituents.

The results reported here demonstrated, for the first time, that dibenzotetraaza[14]annulene derivatives may be of value in research aiming at rational drug design. Further studies of their interactions with various DNA and RNA sequences focused on the potential selectivity as well as biological activity, seem to be of considerable interest.

4. Experimental

4.1. General

Macrocyclic substrates 7,16-bis(hydroxypropyl)-5,14-dihydrodibenzo[*b*,*i*][1,4,8,11]tetraazacyclotetradecine (**1**) and

7,16-bis(2-hydroxybenzoyl)-5,14-dihydrodibenzo[*b*,*i*][1,4,8,11]tetraazacyclotetradecine (**2**) were prepared by the procedures described earlier.[13,14] Other chemicals (diisopropylcarbodiimide (DIC), 4-dimethylaminopyridine (DMAP), tetrabromomethane, bromomethane and triphenylphosphine) were purchased from commercial sources (Sigma–Aldrich, Fluka) and were used as received. Solvents were dried using standard methods and were freshly distilled before use. Elemental analyses were performed on a Euro-EA (EuroVector) microanalyzer. ^{1}H and ^{13}C NMR were run on a Bruker AMX (500 MHz) and a Mercury Varian (300 MHz) spectrometers. Chemical shifts (δ) are expressed in parts per million and *J* values in hertz. Signal multiplicities are denoted as s (singlet), d (doublet), t (triplet), q (quartet) and m (multiplet). ESI mass spectra were taken on a Bruker Esquire 3000 spectrometer. The IR spectra were recorded in KBr with a Bruker IFS 48 spectrophotometer. Melting points were measured with use of a Boethius apparatus and were uncorrected.

4.2. Syntheses

4.2.1. 7,16-Bis[3-(3-pyridyl)propionyloxypropyl]-5,14-dihydrodibenzo[*b*,*i*][1,4,8,11]tetraazacyclotetradecine (3). 3-Pyridinepropionic acid (0.61 g, 4 mmol), DIC (0.65 mL, 4 mmol) and DMAP (0.1 g, 0.82 mmol) were added to a solution of **1** (0.2 g, 0.5 mmol) in dimethylformamide (50 mL). The reaction mixture was protected from moisture and stirred at room temperature for 24 h. The product was precipitated by dropwise addition of water, filtered off and dried under vacuum. Red powder, yield 0.24 g (72%), mp 148 °C. ^{1}H NMR (500 MHz; DMSO-d_6; δ ppm): 1.75 (m, 4H, H^{b}), 2.22 (t, *J*=7.2 Hz, 4H, H^{a}), 2.69 (t, *J*=7.7 Hz, 4H, H^{d}), 2.87 (t, *J*=7.7 Hz, 4H, H^{e}), 4.06 (t, *J*=6.4 Hz, 4H, H^{c}), 6.90 (dd, *J*=6.0, 2.5 Hz, 4H, H^{2,3}, H^{11,12}), 7.26 (m, 6H, H^{1,4}, H^{10,13}, H^{i}), 7.65 (d, *J*=7.8 Hz, 2H, H^{j}), 7.80 (d, *J*=5.9 Hz, 4H, =CHN), 8.39 (dd, *J*=4.7, 1.3 Hz, 2H, H^{h}), 8.45 (d, *J*=1.7 Hz, 2H, H^{g}), 13.57 (t, *J*=5.9 Hz, 2H, NH); ^{13}C NMR (125 MHz; DMSO-d_6; δ ppm): 27.25, 28.36, 30.39, 34.36 (C^{a}, C^{b}, C^{d}, C^{e}), 63.10 (C^{c}), 107.03 (C^{7,16}), 113.64, 123.21, 124.08, 135.61, 135.80, 136.69, 147.24, 147.44, 149.46 (*o*-C_6H_4, C=N, py) 171.91 (C=O); IR (KBr) ν_{max} (cm^{-1}): 3174, 3061, 3030, 2928, 1716, 1652, 1593, 1554; ESI-MS (*m*/*z*): 671.2 (M+H)$^{+}$; Anal. Calcd for $C_{40}H_{42}N_6O_4$: C, 71.62; H, 6.31; N, 12.53. Found: C, 71.20; H, 6.62; N, 12.79%.

4.2.2. 7,16-Bis[3-(*N*-methyl pyridinium-3-yl)propionyloxypropyl]-5,14-dihydrodibenzo[*b*,*i*][1,4,8,11]tetraazacyclotetradecine dibromide dihydrate (4). A solution of **3** (0.19 g, 0.15 mmol) in dimethylformamide (30 mL) was treated with liquid (cooled to −10 °C) bromomethane (5 mL). The mixture was stirred for 24 h under argon at room temperature. The solvent and excess of bromomethane were removed on a rotary evaporator. The oily residue was dissolved in methanol-*tert*-butyl methyl ether (2:5, 70 mL) and left overnight in a refrigerator. The reddish-brown crystals were collected by filtration and dried in vacuo. Yield 0.1 g (75%), mp 223 °C. ^{1}H NMR (300 MHz; DMSO-d_6; δ ppm): 1.78 (m, 4H, H^{b}), 2.27 (t, *J*=6.9 Hz, 4H, H^{a}), 2.83 (t, *J*=7.5 Hz, 4H, H^{d}), 3.05 (t, *J*=7.5 Hz, 4H, H^{e}), 4.08 (t, *J*=6.5 Hz, 4H, H^{c}), 4.31 (s, 6H, H^{k}), 6.90 (dd, *J*=6.1 Hz, *J*=3.5 Hz, 4H, H^{2,3}, H^{11,12}), 7.28 (dd, *J*=6.1, 3.5 Hz, 4H, H^{1,4}, H^{10,13}), 7.83 (d, *J*=5.9 Hz, 4H, =CHN), 8.04 (dd, *J*=6.0, 8.0 Hz, 2H, H^{i}), 8.48 (d, *J*=8.0 Hz, 2H, H^{j}), 8.85 (d, *J*=6.0 Hz, 2H, H^{h}), 9.00 (s, 2H, H^{g}), 13.58 (t, *J*=5.9 Hz, 2H, NH); ^{13}C NMR (75 MHz; DMSO-d_6; δ ppm): 26.82 (C^{e}), 28.31 (C^{a}), 30.42 (C^{b}), 33.13 (C^{d}), 47.70 (C^{k}), 63.42 (C^{c}), 107.07 (C^{7,16}), 113.74 (C^{1,4}, C^{10,13}), 124.18 (C^{2,3}, C^{11,12}), 127.03 (C^{i}), 136.68 (C^{IV}), 140.91 (C^{f}), 143.21 (C^{h}), 144.73 (C^{j}), 145.03 (C^{g}), 147.57 (C=N), 171.61 (C=O); IR (KBr) ν_{max} (cm^{-1}): 3382, 3072, 2898, 1722, 1640, 1589, 1546, 1509, 1451, 1418, 1399, 1357, 1284, 1217, 1157; ESI-MS (*m*/*z*): 350.2 ($C_{42}H_{48}N_6O_4^{2+}$/2); Anal. Calcd for $C_{42}H_{48}Br_2N_6O_4\cdot 2H_2O$: C, 56.26; H, 5.84; N, 9.37. Found: C, 56.39; H, 5.94; N: 9.35%.

4.2.3. 7,16-Bis[2-(3-pyridyl)carbonyloxybenzoyl]-5,14-dihydrodibenzo[*b*,*i*][1,4,8,11]tetraazacyclotetradecine (5). A reaction mixture was prepared containing **2** (0.2 g, 0.38 mmol), nicotinic acid (0.47 g, 3.8 mmol), DIC (0.6 mL, 3.8 mmol) and DMAP (0.1 g, 0.82 mmol) in dimethylformamide (50 mL). Further procedure was analogous to that of **3**. Orange powder, yield 0.25 g (87%), mp 263 °C. ^{1}H NMR (300 MHz; $CDCl_3$; δ ppm): 7.11 (dd, *J*=3.5, 6.1 Hz, 4H, H^{2,3}, H^{11,12}), 7.19 (dd, *J*=3.5, 6.1 Hz, 4H, H^{1,4}, H^{10,13}), 7.33–7.45 (m, 6H, *o*-C_6H_4', H^{d}), 7.54–7.63 (m, 4H, *o*-C_6H_4'), 8.31 (dt, *J*=6.2, 3.4 Hz, 2H, H^{e}), 8.53 (d, *J*=6.6 Hz, 4H, =CHN), 8.75 (dd, *J*=4.9, 1.7 Hz, 2H, H^{c}), 9.24 (dd, *J*=2.2, 0.8 Hz, 2H, H^{b}), 14.23 (t, *J*=6.6 Hz, 2H, NH); ^{13}C NMR (75 MHz; $CDCl_3$; δ ppm): 109.89 (C^{7,16}), 115.75, 123.31, 123.40, 124.99, 126.42, 126.81, 129.41, 131.27, 137.57, 147.66, 151.37, 152.78, 154.08 (*o*-C_6H_4, *o*-C_6H_4', C=N, py), 163.90 (O–C=O), 190.97 (C=O); IR (KBr) ν_{max} (cm^{-1}): 3072, 1745, 1654, 1591, 1496, 1450, 1416, 1330, 1270, 1194, 1096, 1076; ESI-MS (*m*/*z*): 739.2 (M+H)$^{+}$; Anal. Calcd for $C_{44}H_{30}N_6O_6$: C, 71.54; H, 4.09; N, 11.38. Found: C, 71.24; H, 4.14; N, 11.52%.

4.2.4. 7,16-Bis[2-(*N*-methyl pyridinium-3-yl)carbonyloxybenzoyl]-5,14-dihydrodibenzo[*b*,*i*][1,4,8,11]tetraazacyclotetradecine dibromide trihydrate (6). Prepared analogously to **4** starting from **5** (0.1 g, 0.14 mmol) and bromomethane (5 mL). Orange crystals, yield 0.1 g (81%), mp 207 °C. ^{1}H NMR (500 MHz; DMSO-d_6; δ ppm): 4.40 (s, 6H, H^{f}) 7.20 (dd, *J*=3.5, 6.1 Hz, 4H, H^{2,3}, H^{11,12}), 7.32 (dd, *J*=3.5, 6.1 Hz, 4H, H^{1,4}, H^{10,13}), 7.55 (m, 4H, *o*-C_6H_4'), 7.73 (m, 4H, *o*-C_6H_4'), 8.27 (dd, *J*=6.3, 8.0 Hz, 2H, H^{d}), 8.52 (d, *J*=6.6 Hz, 4H, =CHN), 9.02 (d, *J*=8.2 Hz, 2H, H^{e}), 9.25 (d, *J*=6.5 Hz, 2H, H^{c}), 9.68 (s, 2H, H^{b}), 14.17 (t, *J*=6.6 Hz, 2H, NH); ^{13}C NMR (75 MHz; DMSO-d_6; δ ppm): 48.20 (C^{f}), 109.33 (C^{7,16}), 115.71, 123.22, 126.84, 126.96, 127.97, 128.26, 129.68, 131.59, 131.79, 136.01, 144.92, 146.94, 147.15, 149.45, 152.69 (*o*-C_6H_4, *o*-C_6H_4', C=N, py), 160.43 (O–C=O), 189.65 (C=O); IR (KBr) ν_{max} (cm^{-1}): 3398, 3009, 2923, 1747, 1644, 1617, 1591, 1498, 1308, 1267, 1194, 1090; ESI-MS (*m*/*z*): 384.2 ($C_{46}H_{36}N_6O_4^{2+}$/2); Anal. Calcd for $C_{46}H_{36}Br_2N_6O_6\cdot 3H_2O$: C, 56.22; H, 4.31; N, 8.55. Found: C, 56.52; H, 4.14; N, 8.38%.

4.2.5. 7,16-Bis(3-bromopropyl)-5,14-dihydrodibenzo-[*b*,*i*][1,4,8,11]tetraazacyclotetradecine (7). Compound **1** (0.4 g, 1 mmol) was dissolved in warm tetrahydrofuran (250 mL). The solution was allowed to cool to room

temperature and then was treated with tetrabromomethane (1.33 g, 4 mmol) and triphenylphosphine (1.05 g, 4 mmol). The reaction mixture was stirred for 24 h at room temperature, concentrated on a rotary evaporator to half volume, transferred to a separatory funnel and diluted with chloroform (200 mL). The mixture was washed thoroughly with cold water (5×50 mL), dried over anhydrous $CaCl_2$, concentrated to a small volume and left in a refrigerator overnight. Dark-red crystalline product was collected by filtration and dried under vacuum. Yield 0.29 g (55%), mp 217 °C. ^{1}H NMR (500 MHz; DMSO-d_6; 50 °C; δ ppm): 2.16 (m, 4H, H^b), 2.49 (t, J=6.9 Hz, 4H, H^a), 3.68 (t, J=6.6 Hz, 4H, H^c), 7.03 (dd, J=6.0, 3.6 Hz, 4H, $H^{2,3}$, $H^{11,12}$), 7.38 (dd, J=6.0, 3.6 Hz, 4H, $H^{1,4}$, $H^{10,13}$), 7.95 (br s, 4H, =CHN), 13.69 (br s, 2H, NH); ^{13}C NMR (125 MHz; DMSO-d_6; 50 °C; δ ppm): 31.01, 34.54, 35.05 (C^a, C^b, C^c), 107.03 ($C^{7,16}$), 114.23 ($C^{1,4}$, $C^{10,13}$), 124.68 ($C^{2,3}$, $C^{11,12}$), 137.35 (C^{IV}), 148.06 (C=N); IR (KBr) ν_{max} (cm^{-1}): 3168, 3068, 2954, 2885, 1650, 1593, 1554, 1451, 1423, 1401, 1357, 1340, 1314, 1296, 1218, 1160; MALDI-MS (*m*/*z*): 528.08 (M^+), 530.08 $(M+2)^+$; Anal. Calcd for $C_{24}H_{26}Br_2N_4$: C, 54.36; H, 4.94; N, 10.57. Found: C, 54.58; H, 5.12; N, 10.47%.

4.2.6. 7,16-Bis[3-(*N*-pyridinium-1-yl)propyl]-5,14-dihydrodibenzo[*b*,*i*][1,4,8,11]tetraazacyclotetradecine dibromide trihydrate (8). Pyridine (5 mL) was added to a solution of **7** (0.19 g, 0.19 mmol) in dimethylformamide (50 mL). The reaction mixture was stirred at 45 °C under argon for 48 h. The solution was concentrated to a small volume and diluted with diethyl ether to precipitate the product. Deep-red crystalline product was filtered off, washed thoroughly with chloroform and dried. Yield 0.08 g (63%), mp 253 °C. Crystals suitable for X-ray measurements were grown by slow diffusion of *tert*-butyl methyl ether into the solution of **8** in methanol. ^{1}H NMR (300 MHz; DMSO-d_6; δ ppm): 2.18 (m, 4H, H^b), 2.32 (t, J=6.5 Hz, 4H, H^a), 4.68 (t, J=7.2 Hz, 4H, H^c), 6.92 (dd, J=6.1, 3.5 Hz, 4H, $H^{2,3}$, $H^{11,12}$), 7.28 (dd, J=6.1, 3.5 Hz, 4H, $H^{1,4}$, $H^{10,13}$), 7.86 (d, J=5.9 Hz, 4H, =CHN), 8.16 (dd, J=6.7, 7.8 Hz, 4H, H^e), 8.60 (t, J=7.8 Hz, 2H, H^f), 9.17 (d, J=5.6 Hz, 4H, H^d), 13.57 (t, J=6.0 Hz, 2H, NH); ^{13}C NMR (75 MHz; DMSO-d_6; δ ppm): 28.70, 32.81 (C^a, C^b), 60.43 (C^c), 106.33 ($C^{7,16}$), 113.88 ($C^{1,4}$, $C^{10,13}$), 124.19 ($C^{2,3}$, $C^{11,12}$), 127.89 (C^e), 136.68 (C^{IV}), 144.75, 145.32 (C^d, C^f), 147.62 (C=N); IR (KBr) ν_{max} (cm^{-1}): 3451, 3398, 3046, 3022, 2919, 2851, 1634, 1588, 1539, 1488, 1457, 1420, 1398, 1357, 1288, 1217, 1158, 1002; ESI-MS (*m*/*z*): 264.1 ($C_{34}H_{36}N_6^{2+}$/2); Anal. Calcd for $C_{34}H_{36}Br_2N_6\cdot 3H_2O$: C, 55.00; H, 5.70; N, 11.32. Found: C, 54.75; H, 5.66; N, 11.03% (**8** is slightly hygroscopic; the content of water depends on the sample preparation).

4.2.7. 7,16-Bis{3-[4-(4-pyridyl)*N*-pyridinium-1-yl]-propyl}-5,14-dihydrodibenzo[*b*,*i*][1,4,8,11]tetraazacyclotetradecine dibromide pentahydrate (9). 4,4′-Bipyridyl (0.6 g, 3.8 mmol) was added to a solution of **7** (0.1 g, 0.19 mmol) in dimethylformamide (50 mL) and the mixture was stirred at 45 °C under argon for 48 h. The solvent was partially removed under reduced pressure, water (50 mL) was added and the mixture was washed thoroughly with chloroform (5×50 mL). Aqueous layer was concentrated to half volume and left overnight in a refrigerator. The deep-red crystalline product was filtered off and dried in vacuo. Yield 0.11 g (71%), mp 187 °C. Crystals suitable for X-ray measurements were obtained by slow evaporation of aqueous solution of **9**. ^{1}H NMR (300 MHz; DMSO-d_6; δ ppm): 2.25 (m, 4H, H^b), 2.35 (t, J=6.9 Hz, 4H, H^a), 4.74 (t, J=6.7 Hz, 4H, H^c), 6.90 (dd, J=6.1, 3.5 Hz, 4H, $H^{2,3}$, $H^{11,12}$), 7.23 (dd, J=6.1, 3.5 Hz, 4H, $H^{1,4}$, $H^{10,13}$), 7.76 (d, J=5.9 Hz, 4H, =*CH*N), 7.95 (dd, J=1.7, 4.5 Hz, 4H, H^f), 8.59 (d, J=7.0 Hz, 4H, H^g), 8.81 (dd, J=1.7, 4.5 Hz, 4H, H^e), 9.30 (d, J=7.0 Hz, 4H, H^d), 13.42 (t, J=6.0 Hz, 2H, NH); ^{13}C NMR (75 MHz; DMSO-d_6; δ ppm): 28.92, 32.06 (C^a, C^b), 60.21 (C^c), 106.13 ($C^{7,16}$), 113.82, 121.71, 124.18, 124.95, 136.51, 140.57, 145.31, 147.33, 150.78, 152.01 (*o*-C_6H_4, C=N, bipyridyl); IR (KBr) ν_{max} (cm^{-1}): 3388, 2921, 2853, 1637, 1588, 1543, 1459, 1402, 1354, 1286, 1217, 1179, 1162; ESI-MS (*m*/*z*): 341.1 ($C_{44}H_{42}N_8^{2+}$/2); Anal. Calcd for $C_{44}H_{42}Br_2N_8\cdot 5H_2O$: C, 56.66; H, 5.62; N, 12.01. Found: C, 56.40; H, 5.40; N, 12.19% (**9** is slightly hygroscopic; the content of water depends on the sample preparation).

4.3. Crystallography

Intensity data for the crystal of **8** were collected on a KUMA KM4CCD κ-axis diffractometer equipped with monochromated Mo Kα radiation (λ=0.71073 Å) at room temperature. The data integration and numerical absorption corrections were carried out with the CrysAlis program.[23] Intensity data for the crystal of **9** were collected using a Bruker AXS Smart APEX CCD 3-circle diffractometer with MonoCap capillary and monochromated Cu Kα radiation (λ=1.54178 Å) at a temperature of 90 K. Data collection and data reduction were done with the SMART and SAINT-PLUS programs.[24] Empirical absorption corrections were carried out using the SADABS program.[25] The structures were solved by direct methods by using the SHELXS-97 program.[26] All non-hydrogen atoms were refined anisotropically by full-matrix least-squares based on F^2 using the SHELXL-97 program,[27] and the complete set of reflections. The final geometrical calculations were carried out with the PLATON program.[28] The relevant crystal data and experimental details are summarized in Table 1.

All hydrogen atoms were located from Fourier difference maps, assigned isotropic thermal parameters 1.2 times those of their parent non-H atoms (with the exception of the free refined hydrogen atoms of the water molecules), and included in the refinements as riding atoms with N–H 0.86, C_{sp}–H 0.93 and C^2_{sp}–H 0.97 Å for **8**, and with N–H 0.88, C_{sp}–H 0.95, C^2_{sp}–H 0.95 and O–H 0.84 Å for **9**.

4.4. UV–vis spectroscopy

UV–vis spectra were recorded on a Varian Cary 100 Bio spectrophotometer. The spectroscopic studies were performed in aqueous buffer solution (pH=7, sodium cacodylate buffer, I=0.05 mol dm^{-3}). Under the experimental conditions, absorbance of all studied compounds was proportional to their concentrations. Calf thymus *ct*-DNA was purchased from Aldrich, dissolved in the sodium cacodylate buffer, I=0.05 mol dm^{-3}, pH=7, additionally sonicated and filtered through a 0.45 μm filter and final concentration was determined spectroscopically as the concentration of

phosphates.[29,30] Spectroscopic titrations were performed by adding portions of polynucleotide solution to the solution of the studied compound and allowing to incubate for 90 s; the incubation time necessary for reaching thermodynamic equilibrium was checked for each compound. Titration data were processed by Scatchard equation,[19] all having satisfactory correlation coefficients (>0.999), obtained values for K_s and n are given in Table 4. Thermal melting curves for DNA and their complexes with studied compounds were determined as previously described by following the absorption change at 260 nm as a function of temperature. Absorbance of the ligands was subtracted from every curve, and the absorbance scale was normalized. The T_m values are the midpoints of the transition curves, determined from the maximum of the first derivative and checked graphically by the tangent method. ΔT_m values were calculated subtracting T_m of the free nucleic acid from T_m of the complex. Every ΔT_m value here reported was the average of at least two measurements, the error in ΔT_m is ± 0.5 °C.

5. Crystallographic data

Full details of crystallographic data for the structural analysis has been deposited with the Cambridge Crystallographic Data Centre, CCDC No. 602969 for compound **8** and No. 603881 for compound **9**. Copies of this information can be obtained, free of charge via www.ccdc.cam.ac.uk/data_request/cif.

References and notes

1. Mountford, P. *Chem. Soc. Rev.* **1998**, *27*, 105–115 and references therein.
2. (a) Dzugan, S. J.; Busch, D. H. *Inorg. Chem.* **1990**, *29*, 2528–2532; (b) Arai, T.; Kashitani, K.; Kondo, H.; Sakaki, S. *Bull. Chem. Soc. Jpn.* **1994**, *67*, 705–709; (c) Eilmes, J. *Polyhedron* **1992**, *11*, 581–584 and references therein.
3. (a) Drew, M. G. B.; Jutson, N. J.; Mitchell, P. C. H.; Potter, R. J.; Thompsett, D. *J. Mater. Chem.* **1992**, *2*, 817–822; (b) Lu, Y. W.; Keita, B.; Nadjo, L. *New J. Chem.* **1997**, *21*, 581–588; (c) Gupta, V. K.; Prasad, R.; Kumar, P.; Mangla, R. *Anal. Chim. Acta* **2000**, *420*, 19–27; (d) Rudolph, M.; Dautz, S.; Jäger, E. G. *J. Am. Chem. Soc.* **2000**, *122*, 10821–10830.
4. (a) Honeybourne, C. L. *Tetrahedron* **1973**, *29*, 1549–1557; (b) Ricciardi, G.; Bavoso, A.; Rosa, A.; Lelj, F.; Cizov, Y. *J. Chem. Soc., Dalton Trans.* **1995**, 2385–2389.
5. Cutler, A. R.; Alleyne, C. S.; Dolphin, D. *Inorg. Chem.* **1985**, *24*, 2276–2281 and references therein.
6. See e.g.: (a) Sakata, K.; Saitoh, Y.; Kawakami, K.; Nakamura, N.; Hashimoto, M. *Synth. React. Inorg. Met.-Org. Chem.* **1995**, *25*, 1279–1293; (b) Hardie, M. J.; Malic, N.; Nichols, P. J.; Raston, C. L. *Tetrahedron Lett.* **2001**, *42*, 8075–8079; (c) Eilmes, J.; Ptaszek, M.; Woźniak, K. *Polyhedron* **2002**, *21*, 7–17; (d) Eilmes, J.; Ptaszek, M.; Dobrzycki, Ł.; Woźniak, K. *Polyhedron* **2003**, *22*, 3299–3305.
7. Cotton, F. A.; Czuchajowska, J. *Polyhedron* **1990**, *9*, 2553–2566 and references therein.
8. See e.g.: (a) Fiel, R. J. *J. Biomol. Struct. Dyn.* **1989**, *6*, 1259–1274; (b) Marzillli, L. G. *New J. Chem.* **1990**, *14*, 409–420; (c) Armitage, B. *Chem. Rev.* **1998**, *98*, 1171–1200; (d) McMillin, D. R.; Shelton, A. H.; Bejune, S. A.; Fanwick, P. E.; Wall, R. K. *Coord. Chem. Rev.* **2005**, *249*, 1451–1459; (e) Pasternack, R. F.; Ewen, S.; Rao, A.; Meyer, A. S.; Freedman, M. A.; Collings, P. J.; Frey, S. L.; Ranen, M. C.; de Paula, J. C. *Inorg. Chim. Acta* **2001**, *317*, 59–71; (f) Johnson, D. S.; Boger, D. L.; In *Comprehensive Supramolecular Chemistry*; Atwood, J. L., Davies, J. E. D., MacNicol, D. D., Vögtle, F., Eds.; Pergamon: Oxford, New York, NY, 1996; Vol. 4, Chapter 3, pp 106–107 and references therein; (g) Song, R.; Kim, Y.-S.; Lee, C. O.; Sohn, Y. S. *Tetrahedron Lett.* **2003**, *44*, 1537–1540.
9. (a) Scolaro, L. M.; Romeo, A.; Pasternack, R. F. *J. Am. Chem. Soc.* **2004**, *126*, 7178–7179; (b) Chen, X.; Liu, M. J. *Inorg. Biochem.* **2003**, *94*, 106–113 and references therein; (c) Pasternack, R. F.; Gibbs, E. J.; Collings, P. J.; dePaula, J. C.; Turzo, L. C.; Terracina, A. *J. Am. Chem. Soc.* **1998**, *120*, 5873–5878.
10. (a) Aoki, S.; Kimura, E. *Chem. Rev.* **2004**, *104*, 769–787; Liu, J.; Zhang, H.; Chen, C.; Deng, H.; Lu, T.; Ji, L. *Dalton Trans.* **2003**, 114–119.
11. (a) Weiss, M. C.; Gordon, G.; Goedken, V. L. *Inorg. Chem.* **1977**, *16*, 305–310; (b) Rihs, G.; Sigg, I.; Haas, G.; Winkler, T. *Helv. Chim. Acta* **1985**, *68*, 1933–1935; (c) Azuma, N.; Tani, H.; Ozawa, T.; Niida, H.; Tajima, K. *J. Chem. Soc., Perkin Trans. 2* **1995**, 343–348.
12. (a) Meunier, B. *Chem. Rev.* **1992**, *92*, 1411–1456; (b) Pratviel, G.; Pitié, M.; Périgaud, C.; Gosselin, G.; Bernadou, J.; Meunier, B. *J. Chem. Soc., Chem. Commun.* **1993**, 149–151; (c) Ward, B.; Skorobogaty, A.; Dabrowiak, J. C. *Biochemistry* **1986**, *25*, 7827–7833.
13. Hanke, R.; Breitmaier, E. *Chem. Ber.* **1982**, 1657–1661.
14. Sigg, I.; Haas, G.; Winkler, T. *Helv. Chim. Acta* **1982**, *65*, 275–279.
15. Bailey, P. D.; Mills, T. J.; Pettecrew, R.; Price, R. A.; In *Comprehensive Organic Group Transformation II*; Katritzky, A. R., Taylor, R. J. K., Eds.; Elsevier Pergamon: Amsterdam, 2005; Vol. 5, Chapter 5.06, p 223.
16. Buckley, B. R.; In *Comprehensive Organic Group Transformation II*; Katritzky, A. R., Taylor, R. J. K., Eds.; Elsevier Pergamon: Amsterdam, 2005; Vol. 5, Chapter 5.06, p 131.
17. (a) Katritzky, A. R.; Nowak-Wydra, B.; Marson, C. M. *Chem. Scr.* **1987**, *27*, 477–478; (b) Wagner, A.; Heitz, M.-P.; Mioskowski, C. *Tetrahedron Lett.* **1989**, *30*, 557–558.
18. (a) Desiraju, G. R.; Steiner, T. *The Weak Hydrogen Bond in Structural Chemistry and Biology*; Oxford University Press: New York, NY, 1999; (b) Umezawa, Y.; Tsuboyama, S.; Takahashi, H.; Uzawa, J.; Nishio, M. *Tetrahedron* **1999**, *55*, 10047–10056; (c) Hua, L. Z.; Ying, D. C.; Hui, L. J.; Jiang, L. Y.; Hua, M. Y.; Zeng, Y. X. *New J. Chem.* **2000**, *24*, 1057–1062.
19. (a) Scatchard, G. *Ann. N.Y. Acad. Sci.* **1949**, *51*, 660–672; (b) McGhee, J. D.; Von Hippel, P. H. *J. Mol. Biol.* **1976**, *103*, 679–684.
20. Dougherty, G.; Pilbrow, J. R. *Int. J. Biochem.* **1984**, *16*, 1179–1192.
21. Procházková, K.; Zelinger, Z.; Lang, K.; Kubát, P. *J. Phys. Org. Chem.* **2004**, *17*, 890–897.
22. Lugo-Ponce, P.; McMillin, D. R. *Coord. Chem. Rev.* **2000**, *208*, 169–191.
23. *Xcalibur CCD System, CrysAlis Software System, v. 1.171*; Oxford Diffraction, Ltd: Abingdon, England, 2006.
24. *SMART and SAINT-PLUS: Area Detector Control and Integration Software, v. 5.629 and 6.45*; Bruker Analytical X-ray Instruments: Madison, WI, 2003.
25. Sheldrick, G. M. *SADABS, Program for Area Detector Adsorption Correction, v. 2.10*; Institute for Inorganic Chemistry, University of Göttingen: Göttingen, Germany, 2003.

26. Sheldrick, G. M. *SHELXS-97, Program for solution of crystal structures*; University of Göttingen: Göttingen, Germany, 1997.
27. Sheldrick, G. M. *SHELXL-97, Program for refinement of crystal structures*; University of Göttingen: Göttingen, Germany, 1997.
28. Spek, A. L. *PLATON, A Multipurpose Crystallographic Tool*; Utrecht University: Utrecht, The Netherlands, 2005.
29. Chaires, J. B.; Dattagupta, N.; Crothers, D. M. *Biochemistry* **1982**, *21*, 3933–3940.
30. Palm, B. S.; Piantanida, I.; Žinić, M.; Schneider, H.-J. *J. Chem. Soc., Perkin Trans. 2* **2000**, 385–392.